Available online at www.sciencedirect.com

ScienceDirect

Ceramics International 37 (2011) 2281–2285

CERAMICS
INTERNATIONAL

www.elsevier.com/locate/ceramint

Synthesis and characterization of holmium doped lithium niobate powders

F.Z. Fadil [a,b], M. Aillerie [a,*], T. Lamcharfi [b], F. Abdi [b]

[a] Laboratoire Matériaux Optiques, Photonique et Systèmes, Université Paul Verlaine-Metz & Supélec, 2 rue E. Belin, 57070 Metz, France
[b] Laboratoire Signaux Systèmes et Composants, Université Sidi Mohammed Ben Abdellah, route d'Imouzzer, Faculté des Sciences et Techniques de Fès, BP 2202, Fès, Morocco

Received 26 November 2010; received in revised form 13 December 2010; accepted 14 March 2011
Available online 26 May 2011

Abstract

Holmium doped lithium niobate (LN:Ho) powders with initial concentration of holmium in the range 0–7 mol% were synthesized by the ceramic powder processing method. Niobium penta-oxide Nb_2O_5, lithium carboxide $LiCO_3$ and holmium oxide Ho_2O_3 with a purity of 99.99% were the starting materials. The phase content and lattice parameters of powders and ceramic pellets were characterized by X-ray diffraction (XRD). To further investigate the quality of the synthesized LN:Ho powders, the scanning electron microscopy (SEM) was used to determine the particle size and the morphology. The main results of this work point out the fact that the ceramic powder processing method is a well adapt method for obtaining high quality LN:Ho ceramics in the holmium concentration range analysed as the $LiNbO_3$ phase is lonely present in the ceramics at the end of the synthesized process and as their grain sizes are regular, with a maximum for the sample doped with 7 mol% of holmium.

Keywords: Lithium niobate; Holmium doping; Ceramics

---

1. Introduction

Lithium niobate ($LiNbO_3$, LN) is an attractive material for nonlinear and integrated optics due to its interesting set of optical and physical properties. Its large electro-optic and nonlinear coefficients offer a high potential for its use in various domains of modern technology such as optical wave guides, optical memories, information storage by holography and electro-optic devices [1–4]. However, when LN crystals are grown from the melt, it exists in a wide composition range and usually presents a large Li_2O deficiency up to 4% with respect to the stoichiometric composition in the congruent crystal [5]. Therefore, a large amount of defects due to anti-sites defects – Nb in Li sites and structural vacancies necessary to obtain the charge neutrality – is present in non-stoichiometric crystals [6]. As a consequence, the LN lattice is a host for incorporation of dopants such as rare earth or metal ions, even in large concentration [7,8]. Indeed, it is known that the physical properties of LN are strongly dependent of both the intrinsic defects related to the non-stoichiometry and extrinsic defects due to impurities or dopants. Accordingly, several investigations have focused on the LN physico-chemical characterization as function of the composition in pure LN and as function the nature and the concentration of single or co-doped LN in order to improve its performance in high-tech applications, including the photorefractive, non-linear optic and laser ones [9–13]. Beside all dopant elements for LN, holmium (Ho) is a promising element for applications and we can expect, combined to the advantageous intrinsic properties of LN samples, an efficient laser oscillation in the infrared region at 2.1 μm range [14–16]. At this wavelength, a transparency window of the atmosphere exists due to a lower absorption of water. For the same reasons, sensors in medicine can be considered associated, as example, in the same LN:Ho based device, a Mach–Zehnder electro-optic modulator allowing a direct numerical treatment of the measured signal and the sensor itself. In these applications where a high long/width ratio is expected to increase the efficiency of the active part of the device, lithium niobate samples growth from high quality powders or ceramics by the classical Czochralski technique or by the original micro-pulling down technique can be used [17]. For the defects controls of LN crystals and to insure a high crystalline quality of the crystals that are embedded in devices,

---

[*] Corresponding author. Tel.: +33 387378565/688590694; fax: +33 387378569.
E-mail address: aillerie@metz.supelec.fr (M. Aillerie).

0272-8842/$36.00 © 2011 Elsevier Ltd and Techna Group S.r.l. All rights reserved.
doi:10.1016/j.ceramint.2011.05.080

the starting point is the care taken in preparation and characterizations of the powder and ceramics, which will be used in the growth process of LN crystals devoting for specific applications. Currently several synthesis methods have been developed to prepare LN powders, including the Pechini method [18], the non-hydrolytic solution routes [19], the sol–gel [20] and the hydrothermal processes [21] and the conventional ceramic powder processing method, i.e. the method creating the solid state reactions between the corresponding oxides or oxides and carbonates at temperatures above 1000 °C [22]. Beside all, the ceramic powder processing method presents the advantage for the preparation of congruent LN powder that it can well control the size and the morphology of the particle. It is not adapted to the preparation of stoichiometric crystals due to the high temperatures used for the initial calcinations and sintered phases of this method. The present work investigates the synthesis of congruent LN powders and ceramics doped with various concentrations of Holmium from 0 to 7 mol% prepared by the ceramic powder processing method. The phase content and lattice parameters of powders and ceramic pellets were characterized by X-ray diffraction (XRD). To further investigate the quality of the synthesized LN:Ho powders, the scanning electron microscopy (SEM) was used to determine the particle size and the morphology.

2. Experimental

2.1. Synthesis of LN powder

In the experiments, niobium penta-oxide Nb_2O_5, lithium carboxide $LiCO_3$ and holmium oxide Ho_2O_3 with a purity of 99.99% (Agfa Aesar) were the starting materials. Eight solutions were prepared from $y = 0$ to 7 mol% of Ho, with $y = Ho_2O_3/(Nb_2O_5 + LiCO_3)$ and the same amount of Nb_2O_5 and $LiCO_3$ as starting materials .The flow chart depicting the synthesis of LN powder by the solid route is presented in Fig. 1.

$LiCO_3$, Nb_2O_5 and Ho_2O_3 powder were used without further purification. In the typical synthesis process of LN powder the first stage consists of a direct blending of the precursors in a mortar agate during 15 min. This solution was calcined at different temperatures. At first it was heated with a heating rate equal to 5°/min up to a plateau at 400 °C during 1 h, followed by a temperature increase with the same heating rate up to the high temperature final plateau maintained at 1000 °C during 22 h. A second grinding is realized to reduce the agglomerates formed during calcination and to refine the powder. The second phase in the powder preparation consists in the incorporation into the powder of a poly-vinylic acid, PVA used as complex reagent. The slurry so obtained was stirred and then dried in air at 60 °C during 24 h in a furnace. A new grinding phase during 10 min insures the uniformity of the as-prepared precipitate.

The samples in pellet shapes were obtained by pressure with a uniaxial pressure equal to 10 tonnes/cm^2. Then, the pellets were sintered according to the following sintering cycle: a first temperature level at 600 °C during 1 h was created for removing the PVA followed by a second level at 1000 °C for 6 h reached with a heating rate 5 °C/min.

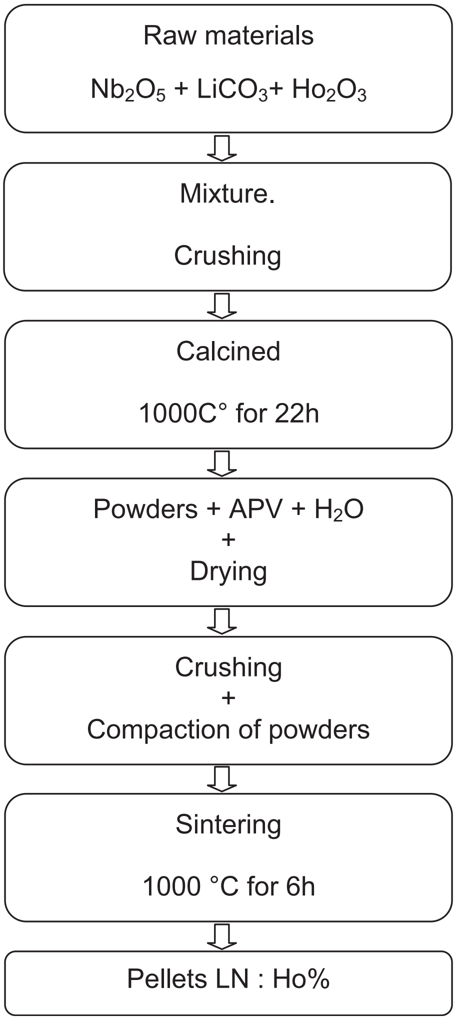

Fig. 1. Flowchart for preparing holmium doped lithium niobate powders by the ceramic powder processing solid method.

2.2. Characterizations

We present in this paper the results of characterizations of the powders synthesized thereby using two techniques: the X-Ray Powder Diffraction (XRD) and the scanning electron microscopy (SEM). These two techniques are commonly used to perform structural characterizations of crystals or powders with the assignation of peaks to elements or phases with the XRD and to determine the grain sizes by observation of the SEM images [20,23,24]. The powder X-ray pattern was recorded for all samples with various holmium concentrations by using a Brucker D8 X-ray diffractometer equipped with a graphite monochromatized Cu Kα radiation. We recorded the XRD spectra in the 2θ range of 20–120° with an increment of 0.01° and a scan speed equal to 0.1 s/step. The window aperture is equal to 20 mm and the sample holder has a rotation speed of 15 rpm. SEM investigations were performed on the microstructure of the obtained LN:Ho ceramics with a JEOL JSM6390 associated to a 0.5–30 KV adjustable Bruker source.

3. Results and discussion

3.1. XRD

XRD patterns of the as-synthesized powders were determined and they are reported as function of the holmium concentration in Fig. 2. The peaks are indexed as the respective planes on the basis of JCPDS cards. Referred to this indexation, it can be noted that for the pure congruent sample, i.e. [Ho] = 0, all the diffraction peaks are assigned to the hexagonal ferroelectric phase of lithium niobate. Moreover, these peaks are the clear signatures of the good crystallinity of the particles. It is also the case in all doped samples in which holmium in the LN structure appears in the patterns with four additional peaks assigned to a secondary phase $HoNbO_4$, the points added in Fig. 2 show these peaks.

The increasing of these four peaks linked to the secondary phase is accompanied with a change of the shape and of the position of all the peaks of the XRD spectra. In the pure congruent LN sample, we can observe at various positions the coexistence of a main peak followed by a very small one. A clear splitting in two separate peaks presents at each position, with an increase of the smallest one can be observed with the increase of holmium concentration indicating a structural change with holmium incorporation [25].

As example of this splitting, we have enhanced in the inset of Fig. 2, the view of the peaks located in $2\Theta = 33^\circ, \ldots, 45^\circ$ for the pure and 7% holmium doped samples. This change in the shape of the XRD response in the XRD spectra is also accompanied by a decrease of the full width at half maximum, FWHM, of the main observed peaks. Additionally, we observed a non-monotonic displacement of the position of some peaks in the XRD spectra, which confirms the structural changes with Ho incorporation. Indeed, a non-monotonic behaviour with dopant incorporation in LN crystals was observed in structural, but also in physical, optical and electrical properties in numerous doped crystal families [26,27,10]. This behaviour was explained by the non-monotonic charge compensation process, involving a concentration change of intrinsic and extrinsic defects, i.e. niobium antisites, dopant, lithium and niobium vacancies, with dopant concentration [28].

Finally, we calculate by a least square fitting procedure from the X-ray peaks intensities the lattice parameters *a* and *c*. We have reported the evolution of these lattice parameters and the ratio *c*/*a* with holmium concentration in samples in Fig. 3A and B, respectively.

The plots in Fig. 3A clearly show that holmium incorporation induce a lattice deformation with an increase of the *a* and *c* parameters with dopant incorporation. Nevertheless, it is to be of note that the increase of these two lattice parameters, in the studied holmium concentration range (from 0 to 7 mol%) corresponds to a dilatation of the lattice at about 0.09% and 0.05% along *a* and *c*, respectively. This dissymmetry in the dilatation is mainly explained by the huge difference in the

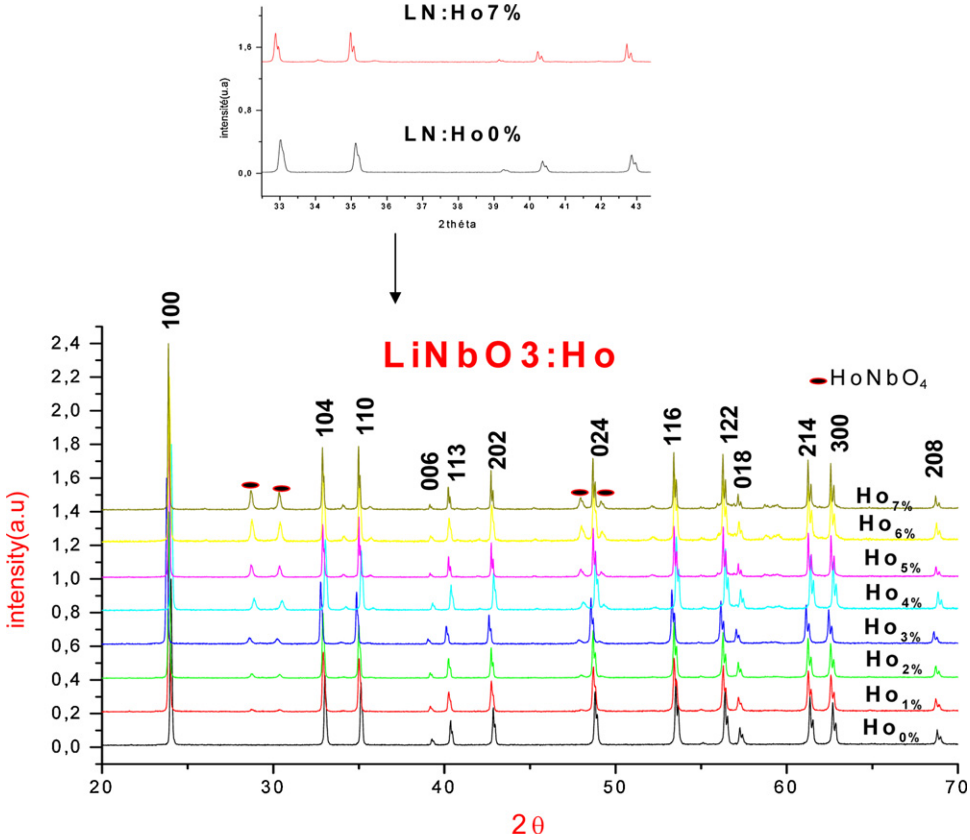

Fig. 2. XRD patterns of the holmium doped lithium niobate powders. Points represent the $NbHoO_4$ crystallographic phase. The view of the peaks located in $2\Theta = 33^\circ, \ldots, 45^\circ$ is enhance in the inset for the pure and 7% holmium doped samples.

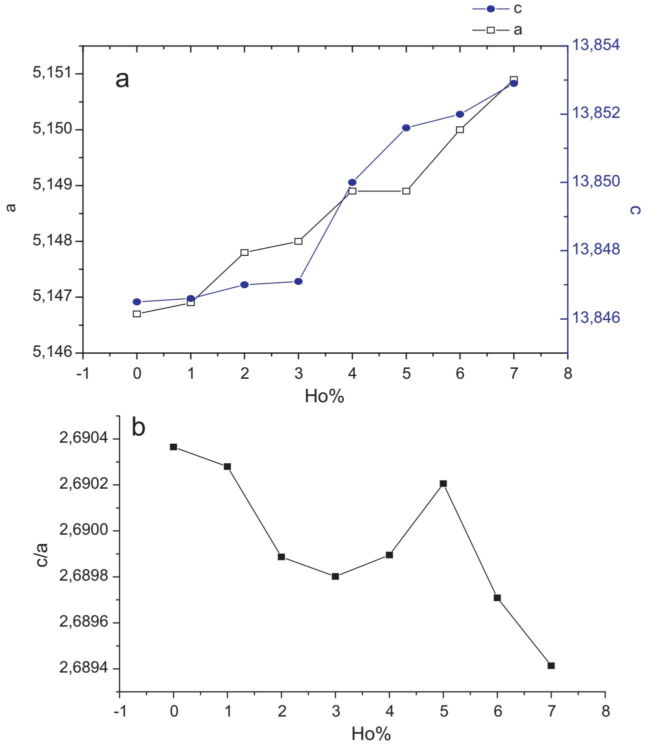

Fig. 3. Evolution of (A) the lattice parameters *a* and *c* of powders and (B) the ratio *c*/*a* with holmium concentration in samples.

absolute initial value of both parameters yielding a larger expansion along the *a* than along the *c* directions, necessary to the incorporation of holmium ions. On the other hand, the *c*/*a* ratio plotted in Fig. 3B, presents a non-linear behaviour with a decrease passing at a minima around 3 mol% followed by an increase up to a maxima located around 5 mol% and a final huge decrease for higher dopant concentration. This behaviour, presenting an horizontal ‘‘S’’ shape, was already observed in some properties of other series of doped LN samples and also attributed to the non-monotonic charge compensation process. Thus, these results obtained in Ho doped LN samples seems to confirm the changes in the charge compensation process with Ho concentration, as invoked above in the direct XRD spectra analysis.

3.2. SEM

SEM images of the synthesized LN pellets are shown in Fig. 4 for the pure congruent and for the 5% and 7% holmium doped lithium niobate samples. The analysis of these pictures allows the study of the microstructure and the comparison of quality and size of the nanocrystals.

The coarsening phenomena observed by SEM, which originates during the sintering process is due to the high strain energy and the large surface area of the nanocrystals [29]. For all samples, we have observed that the fine particles aggregate into grains, which present a quite regular morphology in shape. Assuming particles to be spherical, we calculated that the average particle diameter, reported in Table 1, are in the 3 μm range increasing from 11% in the studied Ho concentration range.

It is to be of note that the well-known Scherrer’s formula, linking the FWHM of peaks in XRD spectra with the particle size deduced of SEM pictures is only valid for grain diameters below 100 nm. Thus, this formula cannot be applied with our ceramics that present an average particle diameter in the 3 μm range. Nevertheless, the non-monotonic evolution of the particle size, Table 1, can be considered as an additional proof of the change in the crystallisation process, which could be attributed to the change in the charge compensation process with Ho incorporation.

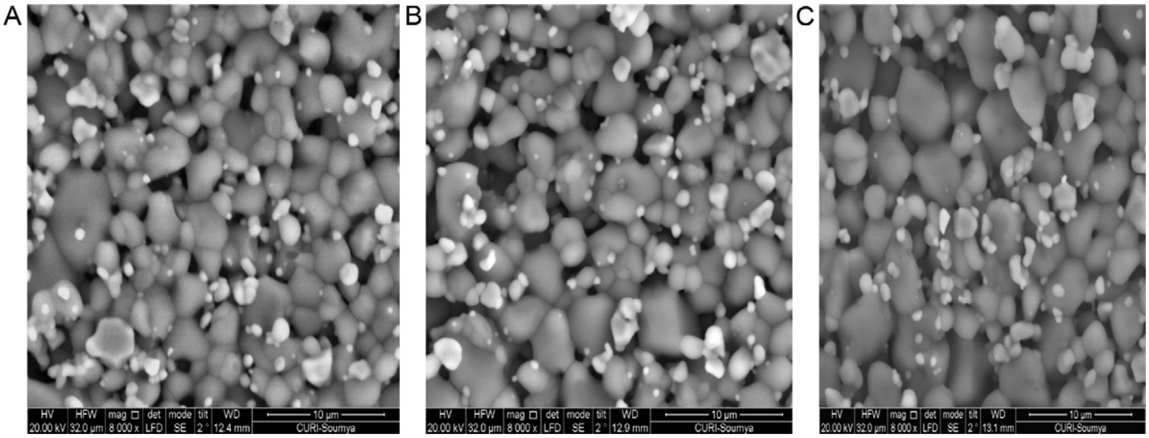

Fig. 4. SEM images of: (A) 0% pure lithium niobate pellet, (B) 5% and (C) 7% holmium doped pellets.

Table 1
Average grainsize of holmium doped lithium niobate pellets.

	0%	1%	2%	3%	4%	5%	6%	7%
$T_{\mathrm{LN:Ho}}$ (μm)	3.09	3.20	3.06	3.19	3.20	3.26	3.25	3.44

4. Conclusion

Holmium doped lithium niobate (LN:Ho) powders with initial concentration of holmium in the range 0–7 mol% were successfully synthesized by the ceramic powder processing solid method. Powders and ceramics in pellet shapes were characterized by X-ray diffraction (XRD) and scanning electron microscopy (SEM).

From XRD, crystallography analysis of these ceramics sintered at 1000 °C during 6 h, indicate that holmium affects the LN lattice by an increase of the lattice parameters *a* and *c*, but a non-monotonic *c*/*a* ratio evolution. From SEM, the analysis shows that the holmium doped LN pellets exhibit relatively uniform grains, and the average grain size of around 3 μm increases non-monotonically by 11% with 7% Ho increase. It is planed that these holmium doped lithium niobate ceramics will be the starting materials for the growth of crystalline fibers by the micro-pulling down technique for applications in infrared. Further structural analysis could confirm the non-monotonic evolution of the observed parameters linked to the compensation charge process.

Acknowledgements

This work was financially supported by the French Centre National de la Recherche Scientifique, CNRS and by the Morocco Centre National de la Recherche Scientifique et Technique, CNRST in the framework of an international cooperation program (CNRST/CNRS SPM 03/08-21620). Authors gratefully acknowledge these institutions.

References

[1] A. Räuber, in: E. Kaldis (Ed.), Current Topics in Material Sciences, vol. 481, North Holland, Amsterdam, 1978.
[2] S. Zhang, Q. Wang, X. Xu, C. Dong, X. Zhang, P. Li, Opt. Laser Technol. 35 (3) (2003) 233–235.
[3] E. Krätzig, O.F. Schirmer, in: P. Günter, J.P. Huignard (Eds.), Photorefractive Materials and their Applications I, vol. 131, Springer, Berlin, 1988.
[4] D. Eimerl, S. Velsko, L. Davis, F. Wang, Prog. Cryst. Growth Charact. Mater. 20 (1990) 59.
[5] F. Abdi, M.D. Fontana, M. Aillerie, P. Bourson, Appl. Phys. A: Mater. Sci. Process. 83 (2006) 427.
[6] F. Jermann, M. Simon, E. Krätzig, J. Opt. Soc. Am. B 12 (1995) 2066.
[7] T. Volk, N. Rubinina, M. Wöhlecke, J. Opt. Soc. Am. B 11 (1994) 1681.
[8] T. Volk, M. Wöhlecke, N. Rubinina, A. Reichert, N. Razumovski, Ferroelectrics 183 (1996) 291.
[9] A. Novoselov, A. Ruso, M. Ferriol, M. Cochez, N. Fressengeas, M. Aillerie, Opt. Mater. 32 (2010) 456–460.
[10] M. Abarkan, M. Aillerie, J.P. Salvestrini, M.D. Fontana, E.P. Kokanyan, Appl. Phys. B 92 (2008) 603–608.
[11] G. Zhong, J. Jin, Z. Wu, in: Proceedings of the 11th Int. Quant. Electronics Conf. IQEC'80, New York, (1980), p. 631.
[12] E.P. Kokanyan, L. Razzari, I. Cristiani, V. Degiorgio, J.B. Gruber, Appl. Phys. Lett. 84 (2004) 1880.
[13] P. Minzioni, I. Cristiani, J. Yu, J. Parravicini, E.P. Kokanyan, V. Degiorgio, Opt. Express 15 (2007) 14171.
[14] A.H. Li, Z.R. Zheng, Q. Lü, L. Sun, Y.H. Xu, W.L. Liu, W.Z. Wu, Y.Q. Yang, T.Q. Lü, J. Appl. Phys. 104 (2008) 063526.
[15] L. McCaughan, D.M. Gill, US Patent 5,227,913 (1993).
[16] G. Dominiak-Dzik, S. Golab, J. Zawadzka, W. Ryba-Romanowski, T. Lukasiewicz, M. Swirkowicz, J. Phys.: Condens. Matter 10 (45) (1998) 10291–10306.
[17] A. Ruso, M. Aillerie, N. Fressengeas, M. Ferriol, Appl. Phys. B 95 (2009) 573–578.
[18] M.P. Pechini, US Patent 3,438,723 (1969).
[19] B.D. Wood, V. Mocanu, B.D. Gates, Adv. Mater. 20 (23) (2008) 4552–4556.
[20] M. Niederberger, N. Pinna, J. Polleux, M. Antonietti, Angew. Chem. 116 (17) (2004) 2320–2323.
[21] C. An, K. Tang, C. Wang, G. Shen, Y. Jin, Y. Qian, Mater. Res. Bull. 37 (2002) 1791.
[22] V.T. Kalinnikov, O.G. Gromov, G.B. Kunshina, A.P. Kuz'min, E.P. Lokshin, V.I. Ivanenko, Inorg. Mater. 4 (2004) 411–414.
[23] L.H. Wang, D.R. Yuan, X.L. Duan, X.Q. Wang, F.P. Yu, Cryst. Res. Technol. 42 (2007) 321–324.
[24] L.N. Wang, X.C. Zhan, Z.G. Zhang, K.L. Zhang, J. Alloys Compd. 456 (1–2) (2008) 461–464.
[25] O. Cerclier, V. Grachev, J. Estienne, J. Phys. IV A 6 (4) (1996) 49–54.
[26] F. Lhommé, P. Bourson, G. Boulon, Y. Guyot, R. Burlot-Loison, M.D. Fontana, M. Aillerie, G. Malovichko, J. Lumin. 83–84 (1999) 441–445.
[27] K. Chah, M. Aillerie, M.D. Fontana, G. Malovichko, K. Betzler, E. Kokanyan, Opt. Commun. 136 (1997) 231–234.
[28] F. Abdi, M. Aillerie, P. Bourson, M.D. Fontana, J. Appl. Phys. 106 (2009) 033519.
[29] C. Burda, X. Chen, R. Narayanan, M.A. EI-Sayed, Chem. Rev. 105 (2005) 1025–1102.